Colloid Polym Sci (2007) 285:985–998
DOI 10.1007/s00396-007-1644-6

ORIGINAL CONTRIBUTION

Drag on two nonuniformly structured flocs moving along the axis of a cylindrical tube

Jyh-Ping Hsu · Shu-Jen Yeh · Shiojenn Tseng

Received: 6 November 2006 / Accepted: 26 December 2006 / Published online: 20 February 2007

Abstract The boundary effect on the drag on two identical, nonuniformly structured flocs moving along the axis of a cylindrical tube filled with a Newtonian fluid is investigated at a small to medium larger Reynolds number. A two-layer model is adopted to simulate various possible structures of a floc, and the flow field inside is described by Darcy–Brinkman model. The results of numerical simulation reveal that a convective flow is present in the rear region of a floc when Reynolds number is on the order of 40. The presence of the tube wall and/or the porous structure of a floc has the effect of reducing that convective flow. For a fixed level of the volume-average permeability of a floc, the influence of the tube wall on the drag depends upon floc structure; the influence on a nonuniformly structured floc is more significant than that on a uniformly structured floc. The more nonuniform the floc structure, the more appreciable the deviation of the drag coefficient–Reynolds number curve from a Stokes'-law-like relation becomes. The smaller the volume-average permeability of a floc and/or the smaller the separation distance between the two flocs, the greater is the deviation, but the presence of the tube wall has the effect of reducing that deviation.

Keywords Drag on two flocs · Nonuniformly structured · Boundary effect · Flocs in cylindrical tube

J.-P. Hsu (✉) · S.-J. Yeh
Department of Chemical Engineering,
National Taiwan University,
10617 Taipei, Taiwan
e-mail: jphsu@ntu.edu.tw

S. Tseng
Department of Mathematics, Tamkang University,
Tamsui,
25137 Taipei, Taiwan

Introduction

The drag on a particle as it moves in a fluid is of both fundamental and practical significance in various fields. Typical example includes sedimentation of particles, fluid flow through packed beds, and fluidized bed operation, to name a few. In practice, the drag on a particle when the influence of nearby particles is significant deserves detailed study. This arises from the fact that experiments and/or operations are often conducted under conditions where many particles are present, and therefore, considering that the behavior of an isolated particle is unrealistic. Apparently, the hydrodynamic interaction between particles needs to be considered, and the separation distance between particles plays a key role. The hydrodynamic interaction between two particles in a Newtonian fluid in the creeping flow regime was discussed thoroughly by Kim and Karrila [1]. Often, the method of reflections was adopted to investigate that interaction between two or more particles [2–4]. Stimson and Jeffery [5] showed that the drag on each of the two rigid, coaxial spheres in an infinite viscous fluid is the same under creeping flow condition. Rowe and Henwood [6] studied the drag on two interacting rigid spheres in an infinite fluid for Reynolds number smaller than 1,000. The influence of a neighboring sphere on the drag on a sphere in an infinite fluid for Reynolds number around 10^4 was investigated by Lee [7]. Tsuji et al. [8] measured the hydrodynamic interactions between two spheres in an infinite fluid for Reynolds number ranging from 200 to 1,000. Li et al. [9] estimated the drag on a floc in a floc dispersion. Using an electronic balance on the viscosity-increased flow field, Zhu et al. [10] measured the drag on two interacting rigid spheres in an infinite fluid for Reynolds number lower than 200. Their method was also adopted by Liang et al. [11] and Chen and Wu [12] to measure the drag on two rigid spheres.

Often, the presence of a boundary on the behavior of a particle as it moves in a dispersion medium needs to be considered. The settling of flocs formed in typical wastewater treatment process, for instance, can be influenced by the wall of settling tank. Chhabra [13] studied experimentally the wall effect on the free settling of particles of various shapes in a Newtonian fluid for Reynolds number smaller than 7. The wall effect on the terminal velocity of a rigid sphere in a quiescent Newtonian fluid in a cylindrical tube was analyzed by Chhabra et al. [14] for Reynolds number up to 200, and up to 3×10^5 when the tube wall is absent. Wham et al. [15] considered the moving of a rigid sphere along the centerline of a circular tube for Reynolds number up to 100. They found that the presence of the tube wall has the effect of raising the drag acting on a particle. Based on a reflection method, Greenstein [16] evaluated the drag on two spherical particles translating in a cylindrical tube filled with an incompressible viscous fluid; a correction factor for particle–particle interaction and that for particle–wall interaction were defined, and both are found to be a function of particle–particle distance and particle–wall distance.

Floc formed in practice is of complicated nature; its shape is irregular and has a highly porous, essentially random structure. Various floc structure models were proposed in the literature. These include uniform model [17–21], three-layer model [22], multilayer model, and two-layer model [9, 23–27]. The specific nature of flocs implies that its behavior in a flow field can be very different from that of rigid particles; several attempts were made recently on the former [8–21, 23–27].

In this work, the boundary effect on the drag on porous particles is analyzed by considering two identical, nonuni-

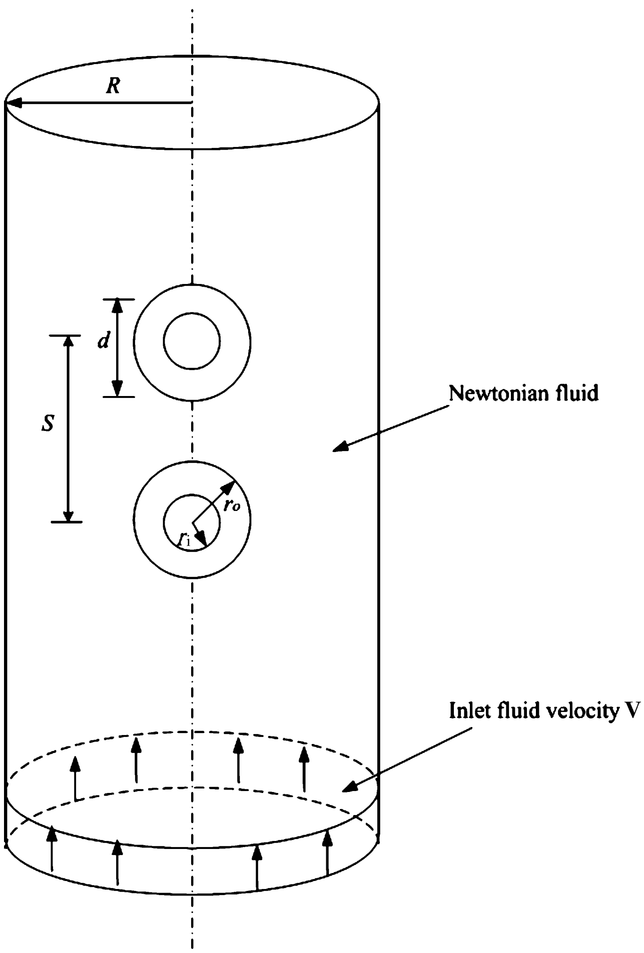

Fig. 1 Schematic representation of the problem considered where two equal-sized, nonuniformly structured flocs are placed on the axis of an infinite cylindrical tube of radius R filled with a Newtonian fluid. d, r_i, r_o, and S are, respectively, the diameter of a floc, the radius of the inner layer of a floc, the radius of the outer layer of a floc, and the center-to-center distance between two flocs. For convenience, the flocs are fixed in the space, and both the bulk liquid and the tube wall move with a relative velocity **V**

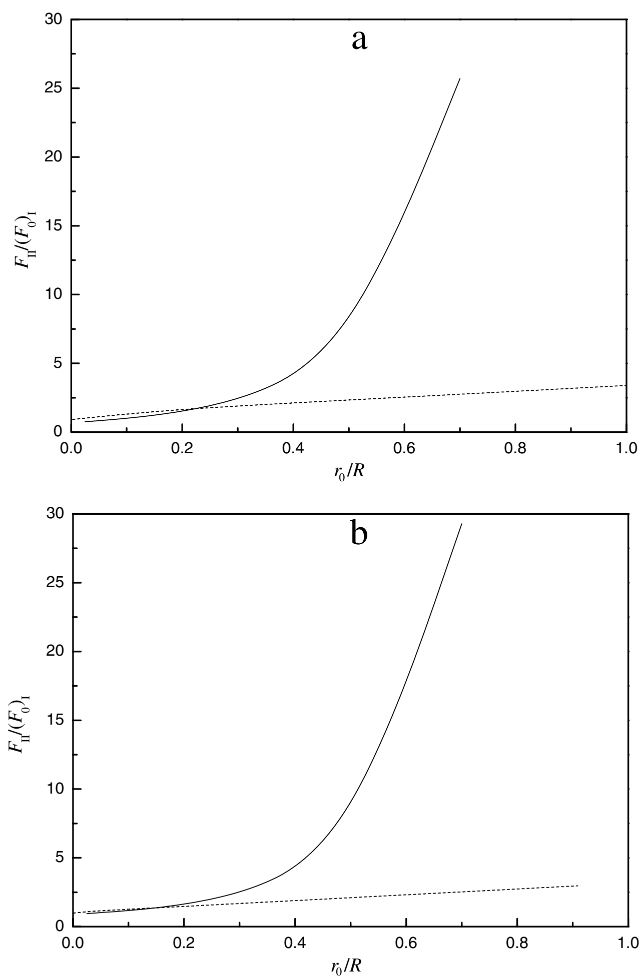

Fig. 2 Variation of scaled drag on two coaxial rigid spheres as a function of (r_o/R) at two levels of (S/d). *Dashed curve* Result of Greenstein [16], *solid curve* present result. **a** S/d=2, **b** S/d=11

formly structured flocs moving along the axis of a cylindrical tube for a small to medium larger Reynolds number. A two-layer model is adopted to simulate various possible structures of a floc, and a Darcy–Brinkman model is used to describe the flow field inside. The influences of the floc tube wall distance, the Reynolds number, the separation distance between two flocs, the relative magnitudes of the permeability of the inner and the outer layers of a floc, and the relative thickness of the inner and the outer layers of a floc on the drag coefficient are examined.

Theory

We consider in this study two identical, nonuniformly structured flocs moving at a steady velocity **V** along the axis of an infinite circular tube of radius R filled with an incompressible Newtonian fluid of constant physical properties. A two-layer model [9, 23–27] is adopted to simulate the structure of a floc. Referring to Fig. 1, let d, r_i and r_o, and S be, respectively, the diameter of a floc, the radii of the inner and the outer layers of a floc, and the center-to-center distance between two flocs. For convenience, the flocs are fixed in the space, and both the bulk liquid and the tube wall move with a relative velocity **V**. Suppose that the system is at a steady state.

For the present case, the flow field in the liquid phase can be described by

$$\mathbf{u_f} \bullet \nabla \mathbf{u_f} = -\nabla P + \frac{2}{Re} \nabla^2 \mathbf{u_f} \tag{1}$$

$$\nabla \bullet \mathbf{u_f} = 0 \tag{2}$$

In these expressions, $Re = 2\rho r_o V_z \big/ \mu_f$ is the Reynolds number, with ρ, μ_f, and V_z being, respectively, the density and the viscosity of fluid and the z-component of **V**. $P = (p + \rho g Z) \big/ \rho V_z^2$ is the scaled pressure: p, g, and Z are, respectively, the pressure, the gravitational acceler-

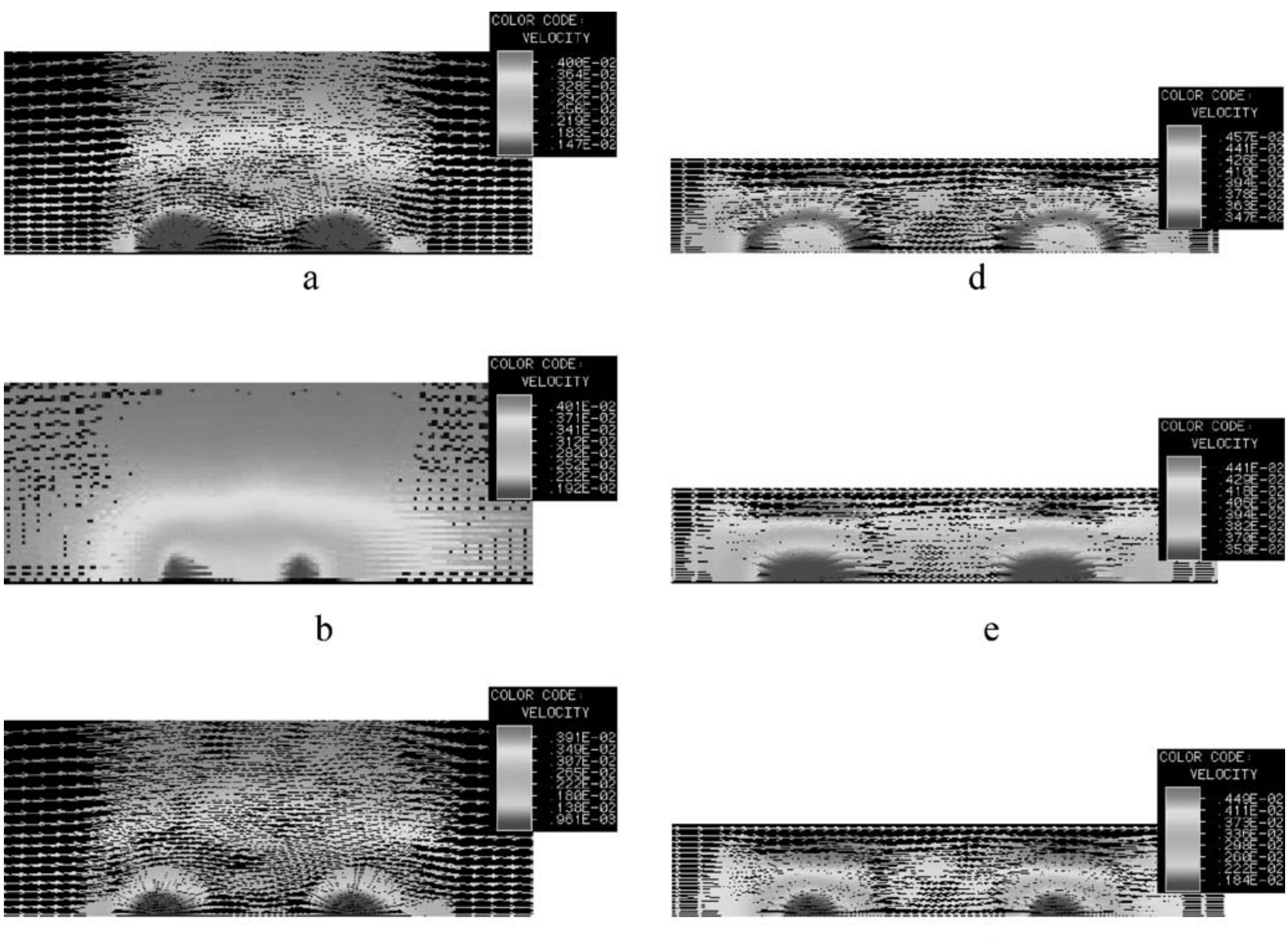

Fig. 3 Flow fields at various combinations of (k_o/k_i) and (r_o/R) at S/d=2, $\overline{\beta}$=2, and Re=0.1. r_o/R=0.1 in (**a**), (**b**), and (**c**), and r_o/R=0.7 in (**d**), (**e**), and (**f**). **a**, **d** k_o/k_i=0.1. **b**, **e** k_o/k_i=1. **c**, **f** k_o/k_i=10

ation, and the z-coordinate. ∇ is the dimensionless gradient operator scaled by $(1/r_o)$, and $\mathbf{u}_f$ is the dimensionless velocity scaled by **V**. Suppose that the flow field inside a floc can be described by Darcy–Brinkman model [28] and the continuity equation. In dimensionless form, we have

$$\mathbf{u_j} + \frac{Re}{2\beta_j^2}\nabla P = \nabla^2 \mathbf{u_j},\ j = o,\ i, \tag{3}$$

$$\nabla \bullet \mathbf{u_j} = 0,\ \ j = o,\ i, \tag{4}$$

In these expressions, j is a region index; j=o and i represent, respectively, the outer and the inner parts of a floc; $\beta_j = r_o/\sqrt{k_j}$ is the scaled floc radius, with k_j being the permeability of region j, and $\mathbf{u}_j$ is the scaled fluid velocity in region j scaled by **V**. The following boundary conditions are assumed:

$$u_z = 1 \text{ on tube wall} \tag{5}$$

$$u_z = 1 \text{ as } z \to \infty \tag{6}$$

$$\mathbf{u_f} = \mathbf{u_o} \text{ and } \mu_f \nabla \mathbf{u_f} = \mu_o \nabla \mathbf{u_o}, r = r_o \tag{7}$$

$$\mathbf{u_o} = \mathbf{u_i} \ \text{ and } \ \mu_o^\bullet \mathbf{u_o} = \mu_i^\bullet \mathbf{u_i}, r = r_i \tag{8}$$

$$\frac{\partial \mathbf{u_f}}{\partial r} = \frac{\partial \mathbf{u_o}}{\partial r} = \frac{\partial \mathbf{u_i}}{\partial r} = 0,\ r = 0 \tag{9}$$

where μ_i and μ_o are, respectively, the viscosity of the liquid in the inner layer of a floc and that in the outer layer of a floc, and u_z is the magnitude of the dimensionless fluid velocity in the z-direction, $\mathbf{u}_z$. Suppose that $\mu_f = \mu_o = \mu_i$. For convenience, we define

$$\overline{\beta} = d_p \Big/ 2\sqrt{\overline{k}} \tag{10}$$

$$\overline{k} = \sum_{j=1}^{2} V_j k_j \Big/ \sum_{j=1}^{2} V_j \tag{11}$$

Here, d_p is the diameter of a particle, $\overline{\beta}$ is a volume-average radius, and $\overline{k}$ is a volume-average permeability. It

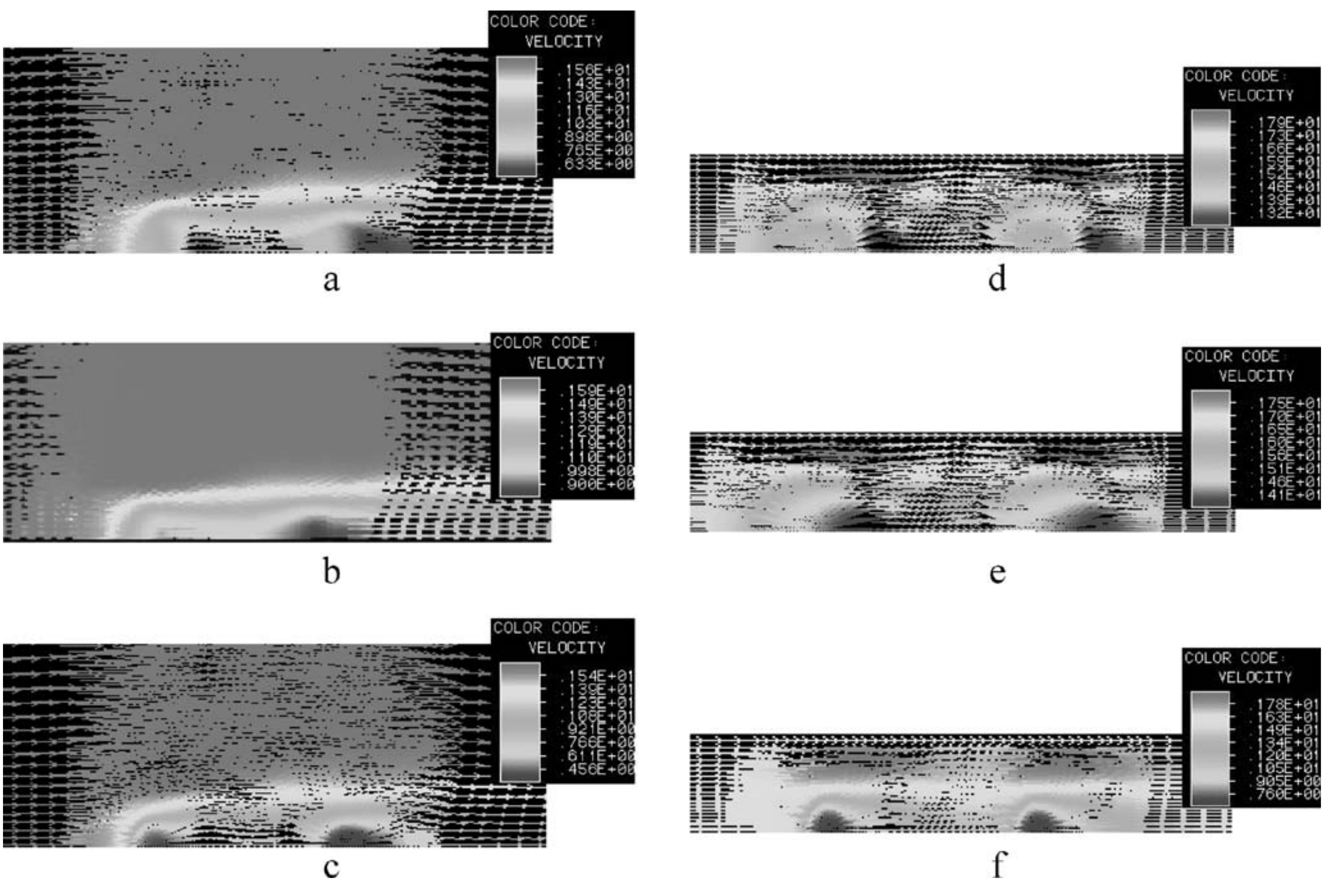

Fig. 4 Flow fields at various combinations of (k_o/k_i) and (r_o/R) at S/d=2, $\overline{\beta}$=2, and Re=40. r_o/R=0.1 in (**a**), (**b**), and (**c**), and r_o/R=0.7 in (**d**), (**e**), and (**f**). **a**, **d** k_o/k_i=0.1. **b**, **e** k_o/k_i=1. **c**, **f** k_o/k_i=10

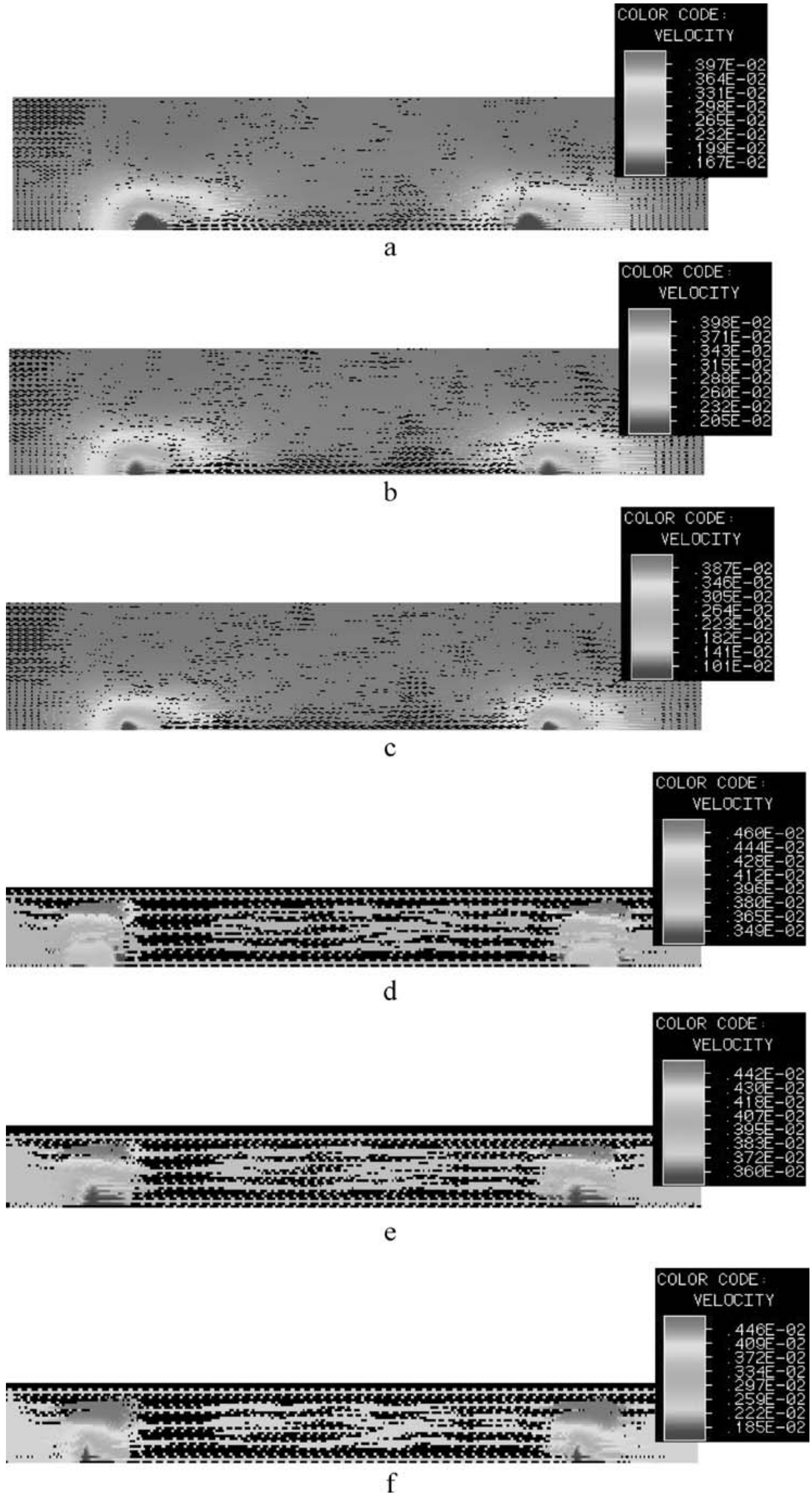

Fig. 5 Flow fields at various combinations of (k_o/k_i) and (r_o/R) at S/d=10, $\overline{\beta}$=2, and Re=0.1. r_o/R=0.1 in (**a**), (**b**), and (**c**), and r_o/R=0.7 in (**d**), (**e**), and (**f**). **a**, **d** k_o/k_i=0.1. **b**, **e** k_o/k_i=1. **c**, **f** k_o/k_i=10

Fig. 6 Flow fields at various combinations of (k_o/k_i) and (r_o/R) at S/d=10, $\overline{\beta}$=2, and Re=40. r_o/R=0.1 in (**a**), (**b**), and (**c**). and r_o/R=0.7 in (**d**), (**e**), and (**f**). **a**, **d** k_o/k_i=0.1. **b**, **e** k_o/k_i=1. **c**, **f** k_o/k_i=10

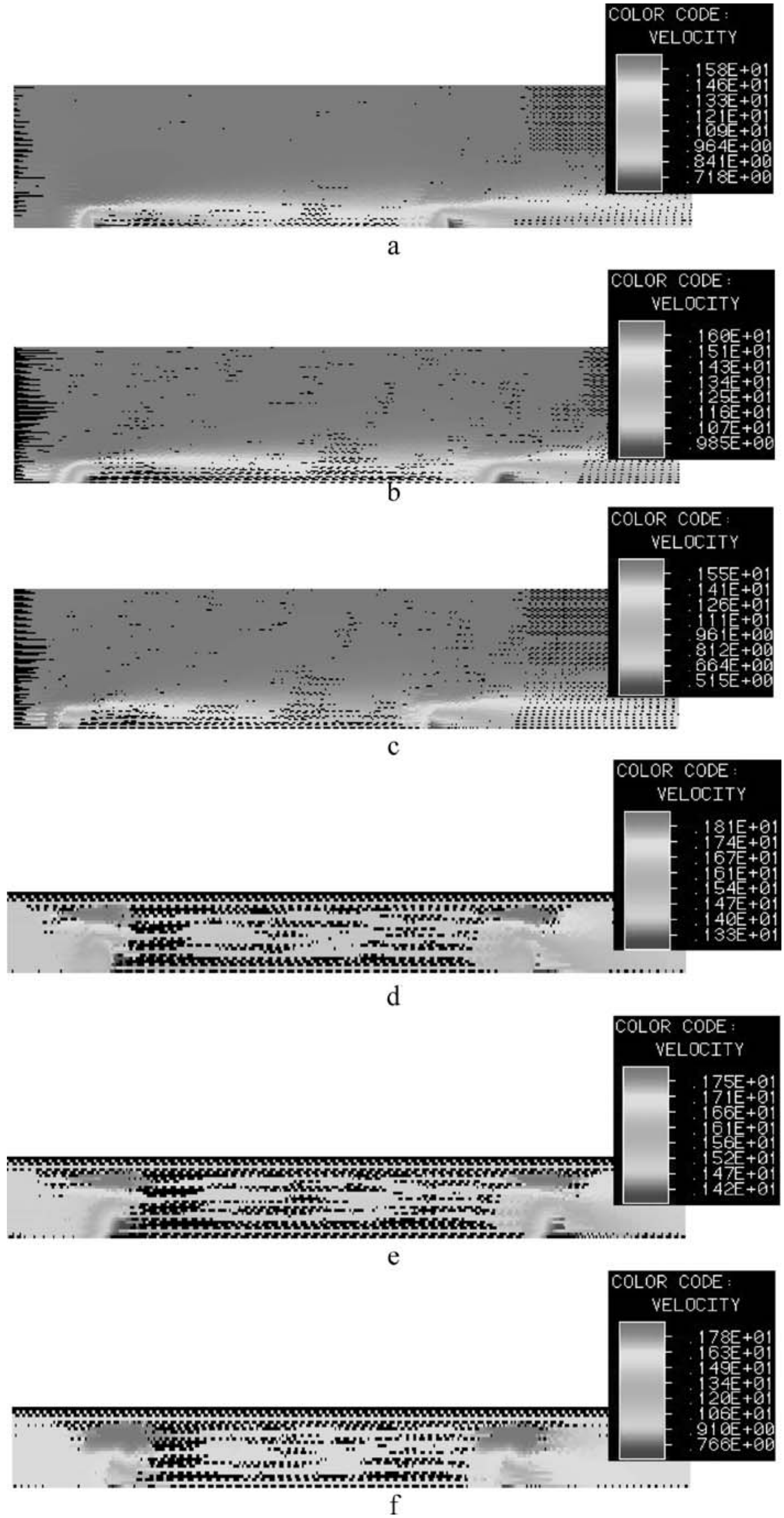

should be pointed out that, depending upon the contents and the formation mechanism, floc can have either a less or more permeable outer layer [29, 30].

Results and discussion

The governing equations and the associated boundary conditions are solved numerically by FIDAP 7.6, a commercial software based on a finite element scheme. The applicability of this software is justified by comparing the present result with that of Greenstein [16], which is based on a reflection method, for the case of two rigid spheres moving along the axis of a circular cylinder at a low Re. Figure 2 shows the variations of $[F_{II}/(F_0)_I]$ as a function of (r_o/R) at two levels of (S/d); $(F_0)_I$ and F_{II} are, respectively, the drag on a single sphere in an unbounded system and the drag on the rear sphere in a bounded system. Note that the results of Greenstein are accurate if the distance both between two spheres and that between sphere and cylinder wall are sufficiently large, that is, both (r_o/S) and (r_o/R) are sufficiently small. Figure 2 reveals that the performance of the present numerical approach is satisfactory.

For illustration, we assume r_o=0.12 cm, r_i=0.06 cm, ρ=1 g/cm^3, and μ=0.01 poise in subsequent discussions. Double precision is used throughout the computation, and grid independence is checked to ensure that the mesh used is fine enough. The numbers of elements used for the liquid phase, the inner layer of a floc, and the outer layer of a floc are 10,032, 30, and 35, respectively.

Flow field

Figures 3 and 4 show the velocity fields for various combinations of (k_o/k_i) and (r_o/R) at two levels of Re for the case when the separation distance between two floc is small; those for the case when it is large are illustrated in

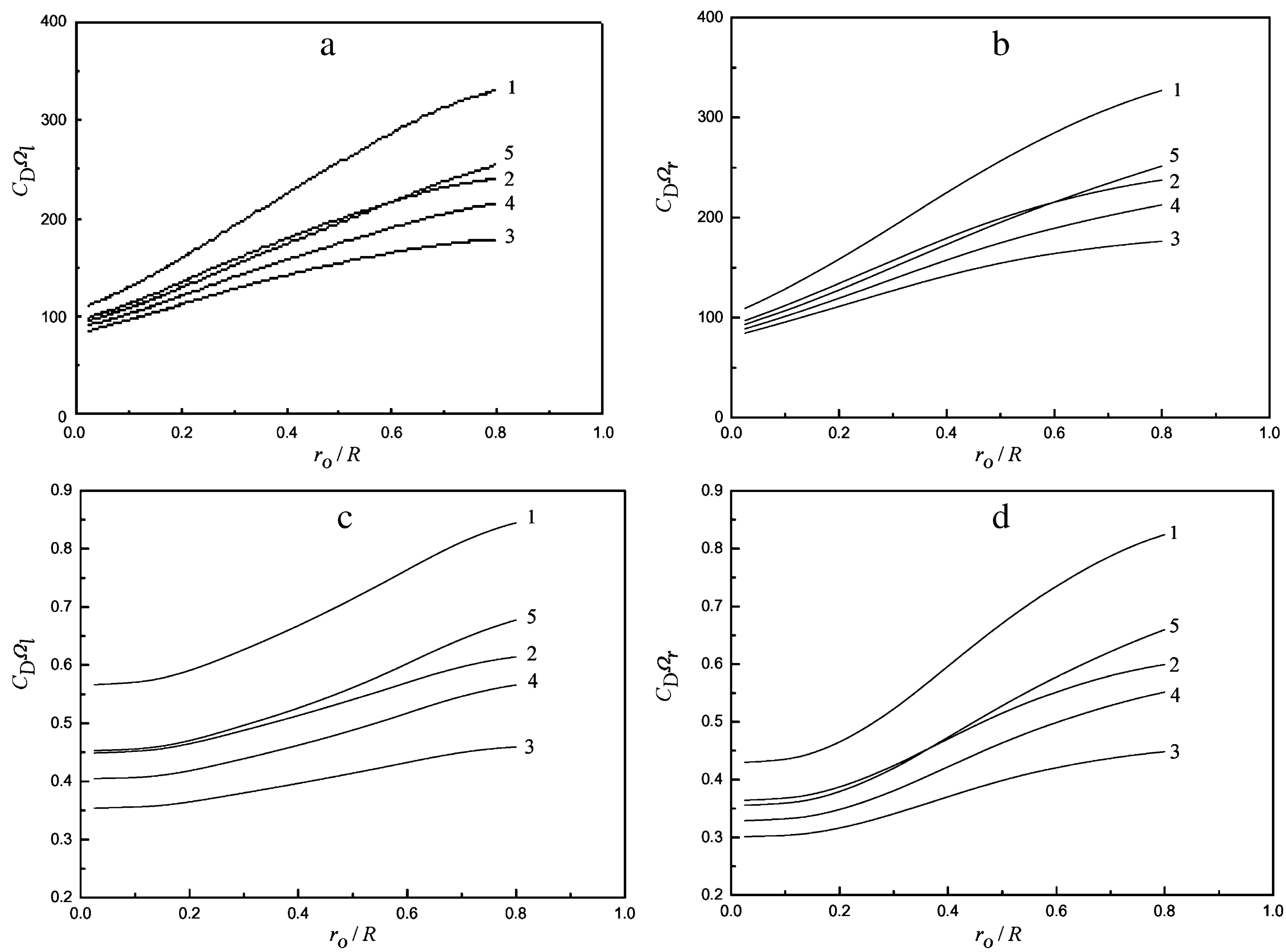

Fig. 7 Variations of $C_D\Omega_l$ (**a**, **c**) and $C_D\Omega_r$ (**b**, **d**) as a function of (r_o/R) for various combinations of (k_o/k_i) and Re at $\overline{\beta}$=2 and S/d=2. *Curves 1* k_o/k_i=0.1, *2* k_o/k_i=0.2, *3* k_o/k_i=1, *4* k_o/k_i=5, *5* k_o/k_i=10. Re=0.1 in (**a**) and (**b**), and Re=40 in (**c**) and (**d**)

Figs. 5 and 6. Note that both the radius and the volume-average permeability of a floc are fixed in these figures. The inner layer of a floc is more permeable than its outer layer in Figs. 3a,d and 4a,d—the reverse is true in Figs. 3c,f and 4c,f—and flocs have a uniform structure in Figs. 3b,e and 4b,e. Figure 3 indicates that if *Re* is small, regardless of the value of (r_o/R), or the influence of the tube wall, the flow field in the upstream of a floc is symmetric to that in its downstream, implying that the convective motion of a fluid is unimportant. However, the nature of the flow field inside a floc is influenced by the presence of the tube wall. For example, Fig. 3d reveals that when the influence of the tube wall is significant, if the inner layer of a floc is more permeable than its outer layer, the flow velocity in the former becomes faster than that in the latter; the reverse behavior is observed in Fig. 3f, where the inner layer of a floc is less permeable than its outer layer. These imply that the prediction of the flow field based on the average permeability of a floc is unreliable. Figure 4 reveals that if *Re* is sufficiently large, the flow field in the upstream region of a floc is no longer symmetric to that in its downstream region, implying that the convective motion of a fluid becomes significant. Under the conditions assumed, due to the high permeability nature of a floc, boundary layer separation is not observed in the downstream region of a floc. Note that the presence of the tube wall has the effect of depressing the degree of asymmetry of the flow field or the convective motion of fluid. Similar behavior was also observed for a rigid particle [31, 32] and a porous particle [25] in a cylinder. The qualitative behaviors of the flow fields in Figs. 5 and 6 are similar to those of Figs. 3 and 4.

Influence of boundary

For the present case, the boundary effect can be measured by the ratio (r_o/R); the larger its value, the more significant

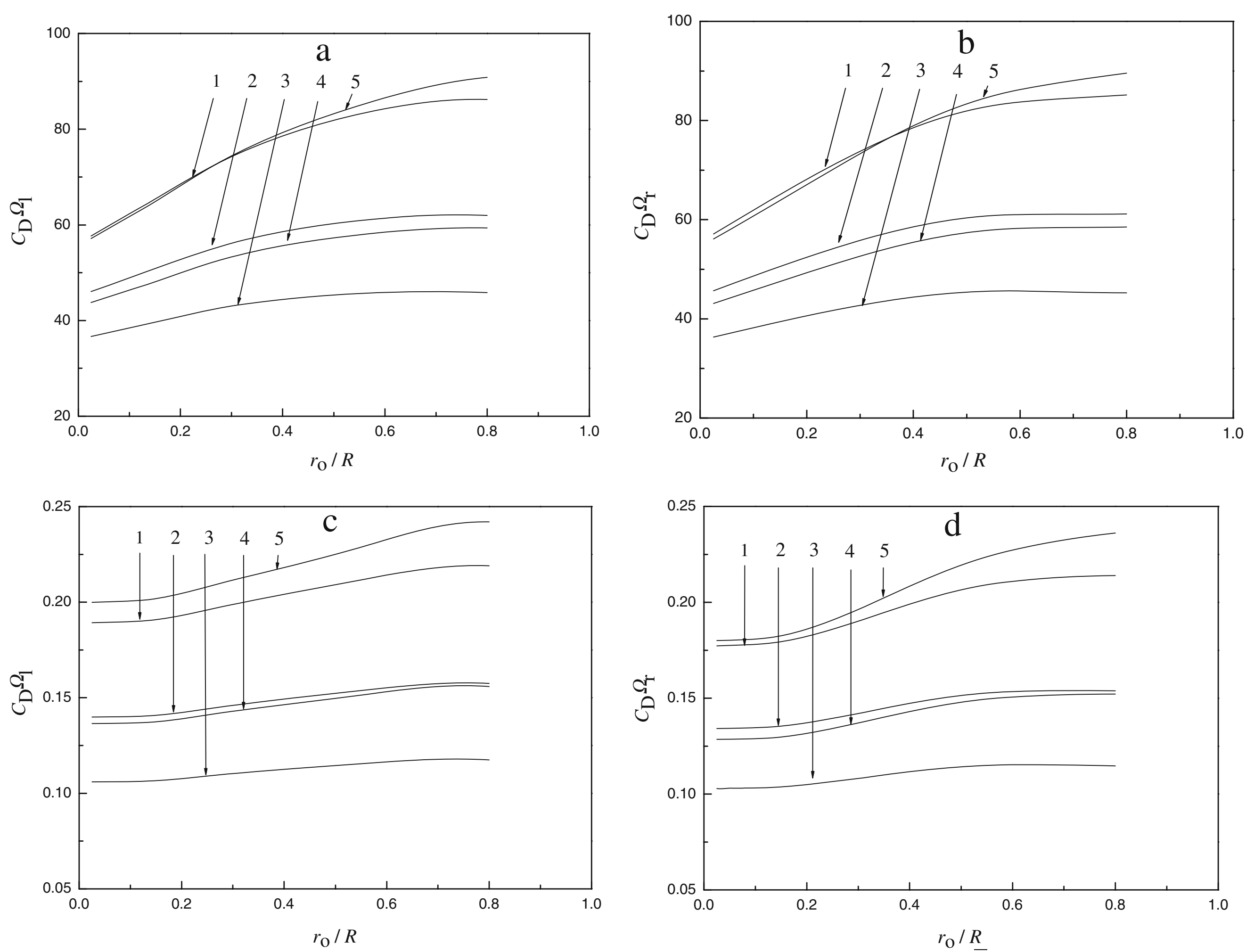

Fig. 8 Variations of $C_D\Omega_l$ (**a**, **c**) and $C_D\Omega_r$, (**b**, **d**) as a function of (r_o/R) for various combinations of (k_o/k_i) and *Re* at $\overline{\beta}$=1 and *S*/*d*=2. *Curves 1* k_o/k_i=0.1, *2* k_o/k_i=0.2, *3* k_o/k_i=1, *4* k_o/k_i=5, *5* k_o/k_i=10. *Re*=0.1 in (**a**) and (**b**), and *Re*=40 in (**c**) and (**d**)

the boundary effect is. Neale et al. [28] proposed using the following expression for a porous sphere of radius r_1 moving with a constant velocity $\mathbf{V}$ in an infinite, stagnant Newtonian fluid of density ρ:

$$\mathrm{F} = \left(\frac{1}{2}\rho V^2\right)\left(\pi r_1^2\right)C_\mathrm{D}\Omega,\ 0 \le \Omega \le 1 \tag{12}$$

where F is the drag on a sphere, C_D is the drag coefficient, and Ω is a correction factor. The variations of $C_\mathrm{D}\Omega$ as a function of (r_o/R) for various combinations of $\overline{\beta}$, (S/d), and (k_o/k_i) at two levels of Re are presented in Figs. 7, 8, and 9. If Re is small, the influence of the leading floc on the rear floc is inappreciable, and the value of $C_\mathrm{D}\Omega_\mathrm{l}$ should close to that of $C_\mathrm{D}\Omega_\mathrm{r}$, which is justified in Figs. 7a,b, 8a,b, and 9a,b. On the other hand, if Re is sufficiently large, wakes are formed in the rear region of the leading floc, and the drag on the rear floc is smaller than that when the leading floc is absent, as can be seen in Figs. 7c,d, 8c,d, and 9c,d. The variations of the ratio $C_D\Omega(r_o/R = 0.7)/C_D\Omega(r_o/R = 0.03)$ illustrated in Table 1 reveal that the influence of the tube wall declines with the increase in Re, increase in the distance between two flocs, and the increase in the volume-average permeability of a floc. Note that even if the volume-average permeability of a floc is fixed, the degree of influence of the tube wall still depends upon its structure, which is consistent with the observation of Wu and Lee [19] and Hsu and Hsieh [25]. For a fixed value of the volume-average permeability, the influence of the tube wall on a uniformly structured floc is less significant than that on a nonuniformly structured floc. The more nonuniform the floc structure, the more important the influence of the tube wall is. For example, $[C_D\Omega(r_o/R = 0.7)/C_D\Omega(r_o/R = 0.03)]$ for $k_\mathrm{o}/k_\mathrm{i}=0.1$ is larger than $[C_D\Omega(r_o/R = 0.7)/C_D\Omega(r_o/R = 0.03)]$ for $(k_\mathrm{o}/k_\mathrm{i}=0.2)$, and $[C_D\Omega(r_o/R = 0.7)/C_D\Omega(r_o/R = 0.03)]$ for $k_\mathrm{o}/k_\mathrm{i}=10$ is larger than $[C_D\Omega(r_o/R = 0.7)/C_D\Omega(r_o/R = 0.03)]$ for $(k_\mathrm{o}/k_\mathrm{i}=5)$.

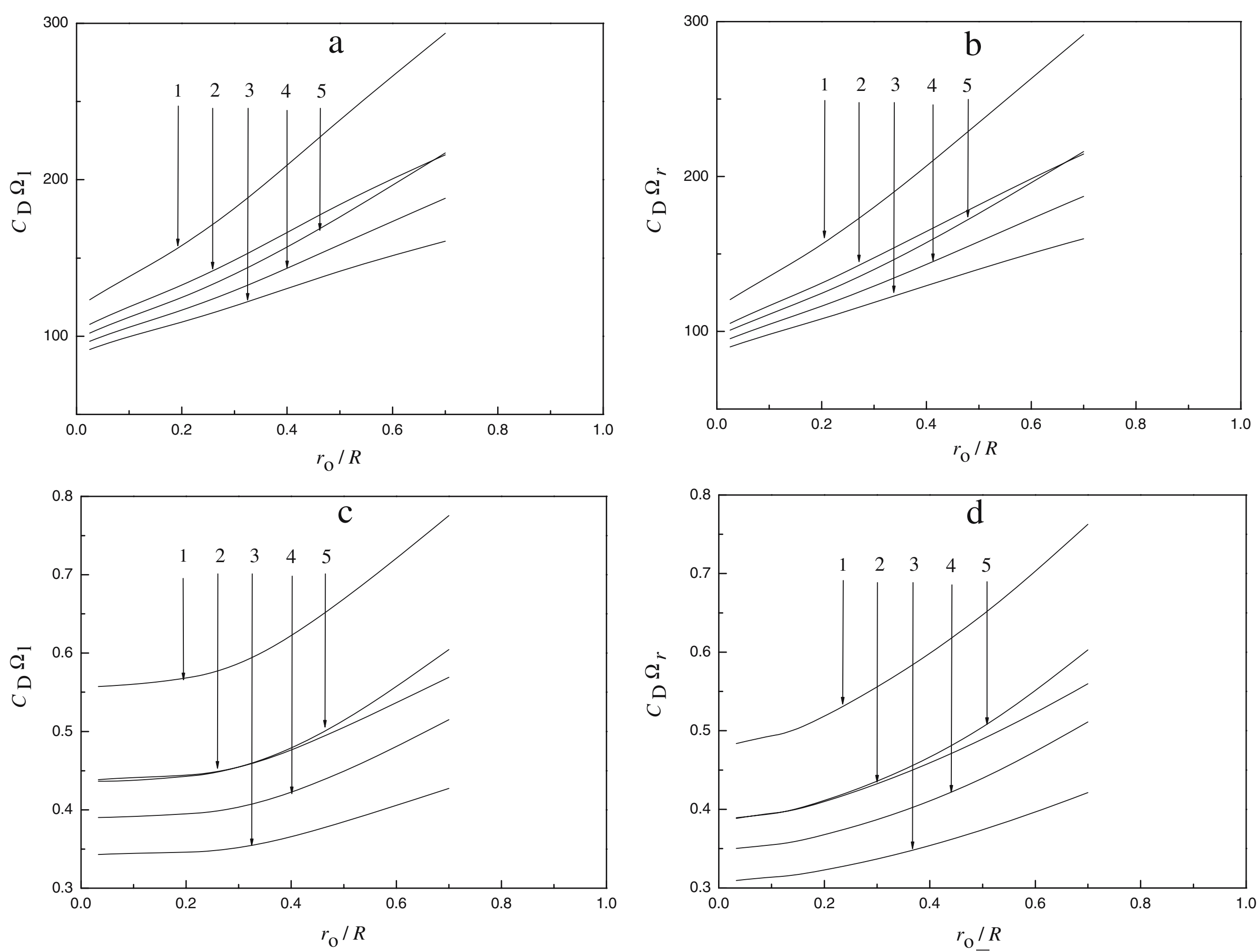

Fig. 9 Variations of $C_D\Omega_l$ (**a**, **c**) and $C_D\Omega_r$, (**b**, **d**) as a function of (r_o/R) for various combinations of $(k_\mathrm{o}/k_\mathrm{i})$ and Re at $\overline{\beta}$=2 and S/d=10. *Curves 1* $k_\mathrm{o}/k_\mathrm{i}$=0.1, *2* $k_\mathrm{o}/k_\mathrm{i}$=0.2, *3* $k_\mathrm{o}/k_\mathrm{i}$=1, *4* $k_\mathrm{o}/k_\mathrm{i}$=5, *5* $k_\mathrm{o}/k_\mathrm{i}$=10. Re=0.1 in (**a**) and (**b**), and Re=40 in (**c**) and (**d**)

Table 1 Influence of boundary on the drag on flocs for various combinations of (*S*/*d*), $\overline{\beta}$, *Re*, and (k_o/k_i)

S/*d*	$\overline{\beta}$	*Re*	k_o/k_i	$C_D\Omega(r_o/R=0.7)/C_D\Omega(r_o/R=0.3)$	
				Leading floc	Rear floc
2	2	0.1	0.1	2.86	2.84
			0.2	2.38	2.36
			1	2.04	2.03
			5	2.28	2.28
			10	2.51	2.52
		40	0.1	1.44	1.84
			0.2	1.34	1.60
			1	1.28	1.46
			5	1.36	1.61
			10	1.43	1.75
2	1	0.1	0.1	1.50	1.48
			0.2	1.35	1.34
			1	1.26	1.25
			5	1.36	1.36
			10	1.57	1.57
		40	0.1	1.16	1.20
			0.2	1.13	1.15
			1	1.12	1.12
			5	1.15	1.18
			10	1.21	1.30
10	2	0.1	0.1	2.38	2.42
			0.2	2.01	2.04
			1	1.76	1.78
			5	1.95	1.96
			10	2.13	2.14
		40	0.1	1.39	1.58
			0.2	1.30	1.44
			1	1.25	1.36
			5	1.32	1.46
			10	1.39	1.55

Influence of Reynolds number

It is known that for the case of a creeping flow around a rigid sphere, the drag coefficient C_D is described by the Stokes' law [33]. For a porous sphere, it can be modified as [25]

$$C_D\Omega = \frac{A(\overline{\beta}, k_o/k_i, r_o/R)}{Re} \tag{13}$$

where *A* is a function of $\overline{\beta}$, (k_o/k_i), and (r_o/R). If this relation exists, then a plot of ln($C_D\Omega$) against ln(*Re*) yields a straight line. In Figs. 10 and 11, ln($C_D\Omega$) is plotted against ln(*Re*) for various values of (k_o/k_i) at two levels of $\overline{\beta}$ for the case when r_o/R=0.1 and r_o/R=0.7. These figures show that the smaller the value of $\overline{\beta}$, the closer a $C_D\Omega$–*Re* curve to a Stokes'-law-like relation. This is realistic because the larger the volume-average permeability of a floc, the more uneasy for wakes to form in its (floc's) rear region. The deviation from a Stokes'-law-like relation also depends upon the magnitude of (r_o/R); the smaller the (r_o/R), the more serious the deviation is. Table 2 summarizes the percentage deviation of $C_D\Omega$ from a Stokes'-law-like relation for various combinations of (r_o/R) and $\overline{\beta}$ at *Re*=40. For fluid flow across a porous floc, because cross flow occurs inside, it is relatively uneasy for wakes to form at its downstream, and, therefore, a Stokes'-law-like relation is applicable to a wider range in *Re*. Table 2 indicates that the deviation of $C_D\Omega$ increases with the increase in $\overline{\beta}$ or the decrease in (r_o/R); the latter implies that the presence of the tube wall has the effect of confining the convective flow near a floc. Table 2 also suggests that the more nonuniform the structure of a floc, the more serious the deviation becomes. Note that all the deviations are positive, and as *Re* increases, the deviation becomes more serious. However, because the rear floc is influenced by the wakes behind the leading floc, the deviation in the $C_D\Omega$ of the former is smaller than that of the latter.

Influence of floc structure

Figure 12 shows the variation of $C_D\Omega$ on each floc as a function of (r_i/r_o) at various values of (k_o/k_i) for the case when r_o/R=0.7 and *Re*=40; the corresponding variation in

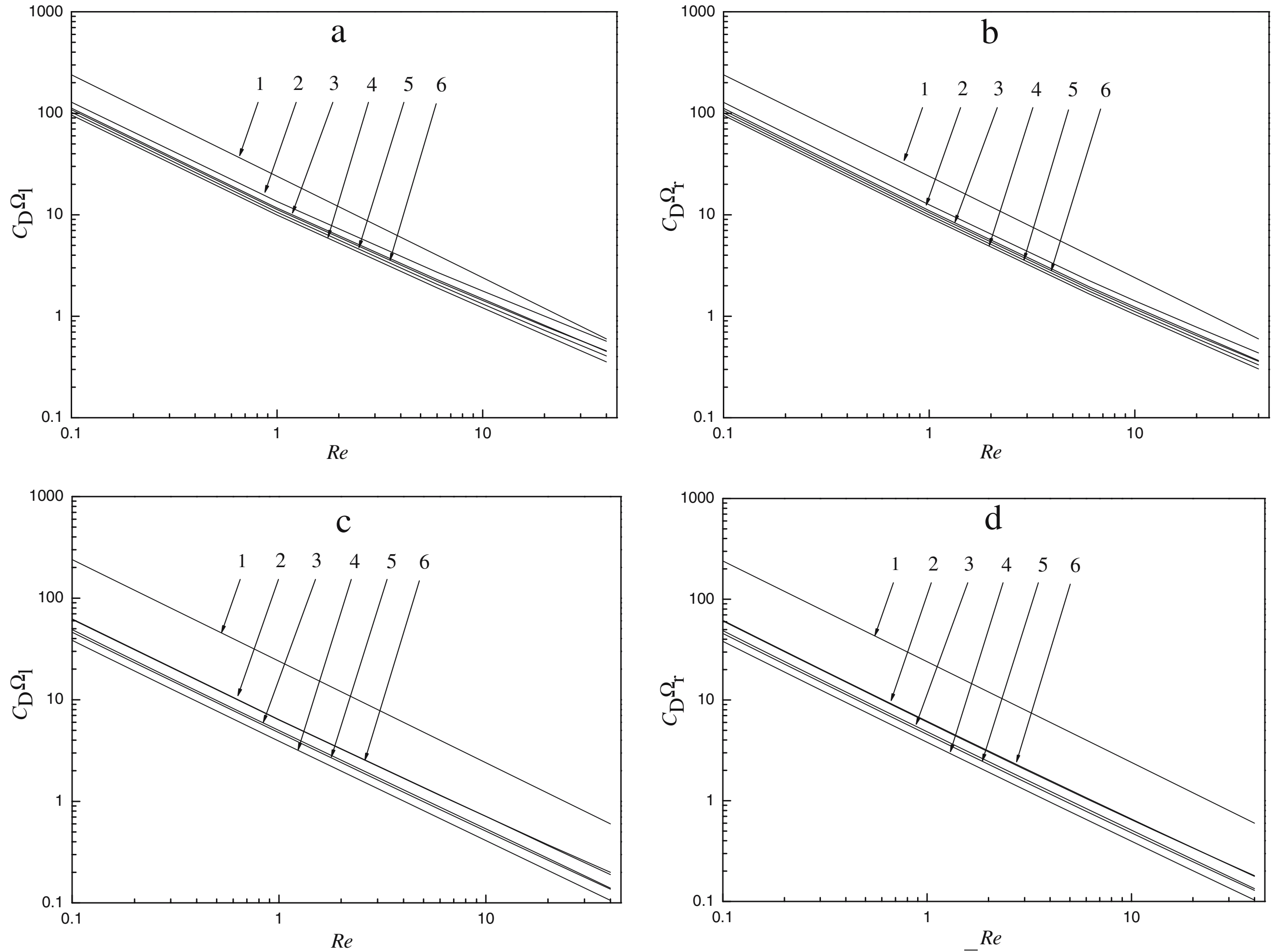

Fig. 10 Variations of $C_D\Omega_l$ (**a**, **c**) and $C_D\Omega_r$ (**b**, **d**) as a function of *Re* for various combinations of (k_o/k_i) and $\overline{\beta}$ at S/d=2 and r_o/R=0.1. *Curves 1* Stokes' law, *2* k_o/k_i=0.1, *3* k_o/k_i=0.2, *4* k_o/k_i=1, *5* k_o/k_i=5, *6* k_o/k_i=10. $\overline{\beta}$=2 in (**a**) and (**b**), and $\overline{\beta}$=1 in (**c**) and (**d**)

the ratio ($C_D\Omega_r/C_D\Omega_l$) is also presented. According to Eq. 10, if $(k_o/k_i)<1$ and the volume-average permeability of a floc remains fixed, then as (r_i/r_o) increases, both the permeability of the outer layer and that of the inner layer of a floc must decrease, which yields a larger $C_D\Omega_l$ and a larger $C_D\Omega_r$. Because the decrease in the permeability of the outer and the inner layers of a floc as (r_i/r_o) increases is appreciable, the corresponding increase in $C_D\Omega$ is substantial (curves 1 and 2 in Fig. 12a,b). On the other hand, if $(k_o/k_i)>1$ as (r_i/r_o) increases, the permeability of both the outer layer and that of the inner layer of a floc must increase, which yields a smaller $C_D\Omega_l$ and a smaller $C_D\Omega_r$. However, because the increase in the permeability of the outer and the inner layers of a floc as (r_i/r_o) increases is inappreciable, so as well is the corresponding decrease in $C_D\Omega$ (curves 4 and 5 in Fig. 12a,b). In particular, we have $C_D\Omega_l(k_o/k_i{=}\ 0.1,r_i/r_o=0.7)=2.99C_D\Omega_l(k_o/k_i{=}\ 0.1,r_i/r_o=0.25)$, $C_D\Omega_l(k_o/k_i{=}\ 0.2,r_i/r_o=0.7)=2C_D\Omega_l(k_o/k_i{=}\ 0.2,r_i/r_o=0.25)$, $C_D\Omega_l(k_o/k_i{=}\ 5,r_i/r_o=0.7)=0.86C_D\Omega_l(k_o/k_i{=}\ 5,r_i/r_o=0.25)$, and $C_D\Omega_l(k_o/k_i{=}\ 10,r_i/r_o=0.7)=0.89\,C_D\Omega_l(k_o/k_i{=}\ 10,r_i/r_o=0.25)$. These also imply that the more nonuniform the structure of a floc, the more significant the influence of (r_i/r_o) is. The degree of increase in $C_D\Omega$ as (r_i/r_o) increases is enhanced by the presence of the tube wall. For example, if the tube wall is absent, $C_D\Omega_l(k_o/k_i{=}\ 0.1,r_i/r_o=0.7)=2.19\,C_D\Omega_l(k_o/k_i{=}\ 0.1,r_i/r_o=0.25)$, $C_D\Omega_l(k_o/k_i{=}\ 0.2,r_i/r_o=0.7)=1.71\,C_D\Omega_l(k_o/k_i=0.2,r_i/r_o=0.25)$, $C_D\Omega_l(k_o/k_i=5,r_i/r_o=0.7)=0.88\,C_D\Omega_l(k_o/k_i=5,r_i/r_o=0.25)$, and $C_D\Omega_l(k_o/k_i{=}\ 10,r_i/r_o=0.7)=0.90\,C_D\Omega_l(k_o/k_i{=}\ 10,r_i/r_o=0.25)$ [29]. The qualitative behavior of $C_D\Omega_r$ is similar to that of $C_D\Omega_l$. Figure 12c suggests that the presence of the tube wall has the effect of reducing the difference between the drag on the leading floc and that on the rear floc. The curves 3 in Fig. 12 are flat because they represent the results for homogeneous flocs.

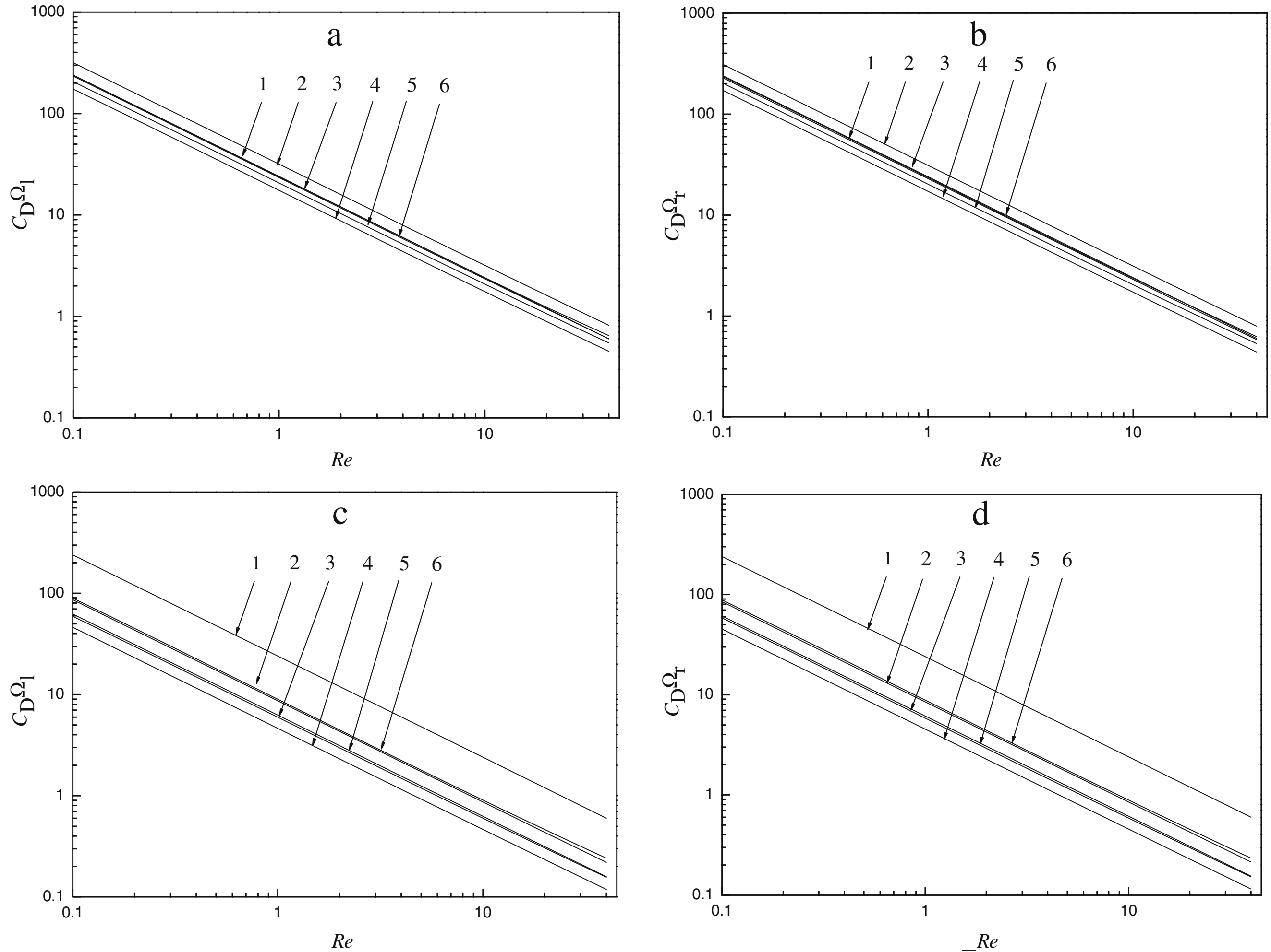

Fig. 11 Variations of $C_D\Omega_l$ (**a**, **c**) and $C_D\Omega_r$ (**b**, **d**) as a function of *Re* for various combinations of (k_o/k_i) and $\overline{\beta}$ at S/d=2 and r_o/R=0.7. *Curves 1* Stokes' law, *2* k_o/k_i=0.1, *3* k_o/k_i=0.2, *4* k_o/k_i=1, *5* k_o/k_i=5, *6* k_o/k_i=10. $\overline{\beta}$=2 in (**a**) and (**b**), and $\overline{\beta}$=1 in (**c**) and (**d**)

Conclusion

The drag on two identical, nonuniformly structured spherical flocs along the axis of a cylindrical tube filled with a Newtonian fluid is evaluated. The governing equations for the flow field coupled with a two-layer model for floc structure are solved numerically for small to medium larger Reynolds numbers. We conclude the following: (a) For uniformly structured flocs at a Reynolds number of 40 if the wall effect is unimportant, the flow field near the upstream region of a floc is asymmetric to that in its downstream region, which arises from the convective flow of fluid. The flow fields become symmetric, however, when the wall effect becomes important. That is, the presence of the tube wall has the effect of compressing the flow fields. This effect is pronounced as the separation distance between two flocs declines. (b) In addition to the effect of the tube wall, whether the convective flow of fluid is important is also influenced by the structure of a floc. (c) For a fixed value of volume-average permeability, the influence of the tube wall on the behavior of a nonuniformly structured floc is more significant than that of a uniformly structured floc, and the degree of influence in the former varies with the nature of floc structure. (d) Regardless of the level of Reynolds number and the separation distance between two flocs, the presence of the tube wall has the effect of raising the drag, which arises from the nonuniform structure of a floc. (e) If the permeability of floc is high, the more significant the wall effect is and the closer the drag coefficient–Reynolds number curve to a Stokes'-law-like relation becomes. The more nonuniform the floc structure, the more appreciable the deviation of the drag coefficient–Reynolds number curve to that relation becomes. (f) If the volume-average permeability of a floc is fixed, the behavior of the drag as the ratio (radius of inner layer/radius of outer layer) varies, when the outer layer of a floc is less permeable than its inner layer, is totally different from that when it is more

Table 2 Percentage deviation from a Stokes'-law-like relation at Re=40 and S/d=2 for various combinations of (r_o/R), $\overline{\beta}$, and (k_o/k_i)

R_o/R	$\overline{\beta}$	k_o/k_i	Percentage deviation (%)	
			Leading floc	Rear floc
0.1	1	0.1	21.766	14.876
		0.2	14.470	10.590
		1	10.277	7.934
		5	17.905	12.515
		10	29.933	18.921
	2	0.1	76.468	35.390
		0.2	60.026	31.198
		1	47.605	26.937
		5	58.742	31.021
		10	68.039	34.159
0.7	1	0.1	1.673	1.017
		0.2	1.648	1.012
		1	2.538	1.716
		5	5.654	4.129
		10	7.775	5.753
	2	0.1	3.197	2.134
		0.2	2.831	1.857
		1	3.490	2.372
		5	6.642	4.805
		10	8.594	6.339

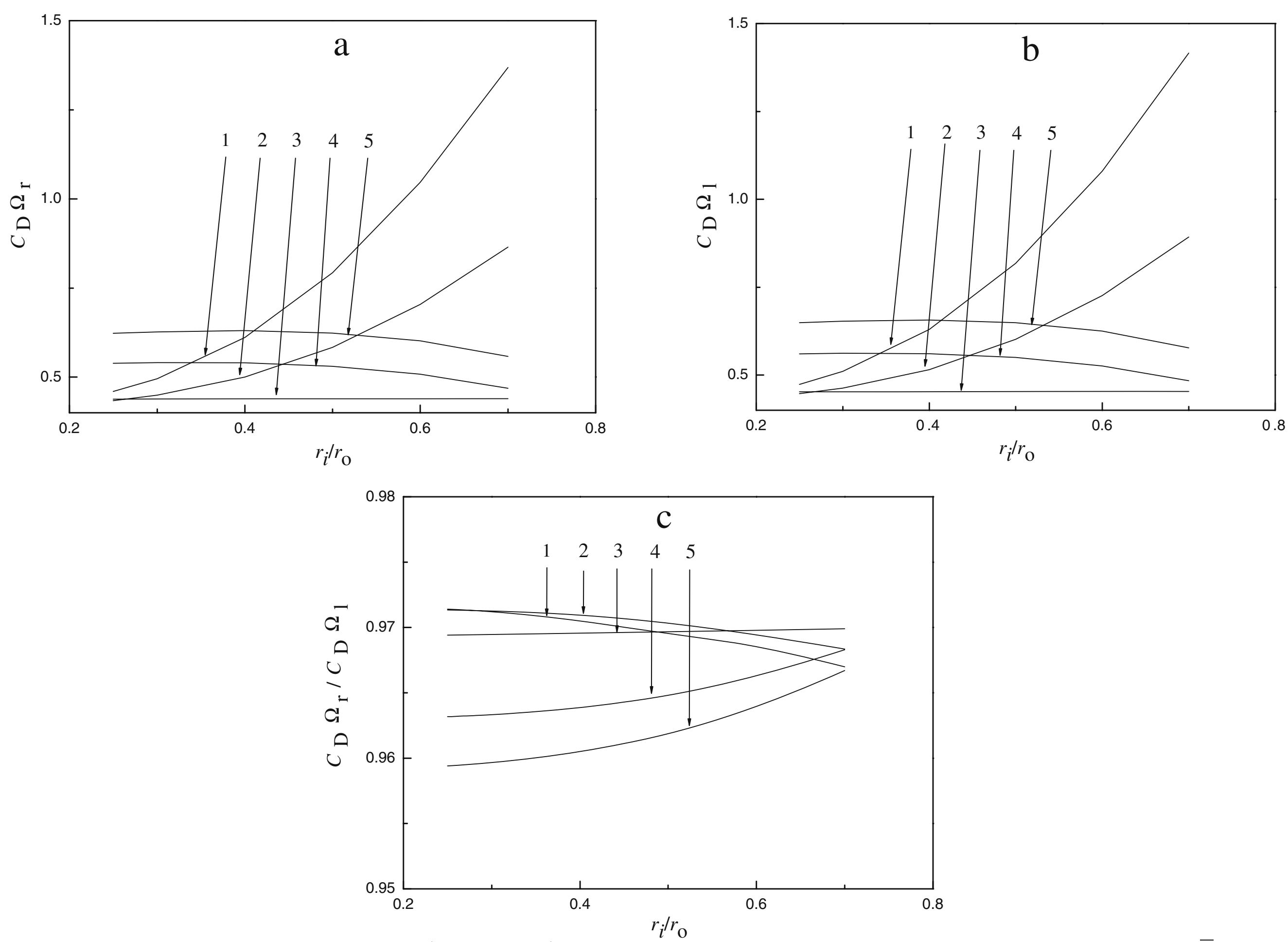

Fig. 12 Variations of $C_D\Omega_r$ (**a**), $C_D\Omega_l$ (**b**), and $(C_D\Omega_r/C_D\Omega_l)$ (**c**) as a function of (r_i/r_o) at various values of (k_o/k_i) at S/d=2, r_o/R=0.7, $\overline{\beta}$=2, and Re=40. *Curves 1* k_o/k_i=0.1, *2* k_o/k_i=0.2, *3* k_o/k_i=1, *4* k_o/k_i=5, *5* k_o/k_i=10

permeable. In general, the influence of the ratio (radius of inner layer/radius of outer layer) on the drag is more important when its inner layer is more permeable than its outer layer; in addition, the more significant the wall effect, the less important the influence of that ratio is.

Acknowledgment This work was supported by the National Science Council of the Republic of China.

References

1. Kim S, Karrila SJ (1991) Microhydrodynamics. Butterworth-Heinemann, Boston, (Chapter 9)
2. Smoluchowski M (1911) Bull Acad Cracow 1A:28
3. Kynch GJ (1959) J Fluid Mech 5:193
4. Happel J, Brenner H (1983) Low Reynolds number hydrodynamics. Academic, New York
5. Stimson M, Jeffery GB (1926) Proc R Soc Lond A 111:110
6. Rowe PN, Henwood GA (1961) Inst Chem Eng 39:43
7. Lee KC (1979) Aerosp Q 30:371
8. Tsuji Y, Morikawa Y, Terashima K (1982) Int J Multiphase Flow 8:71
9. Hsu JP, Li MC, Chang AC (2005) J Colloid Interface Sci 284:332
10. Zhu C, Liang SC, Fan LS (1994) Int J Multiphase Flow 20:117
11. Liang SC, Hong T, Fan LS (1996) Int J Multiphase Flow 22:285
12. Chen RC, Wu JL (2000) Chem Eng Sci 55:1143
13. Chhabra RP (1995) Powder Technol 85:83
14. Chhabra RP, Agarwal S, Chaudhary K (2003) Powder Technol 129:53
15. Wham RM, Basaran OA, Byers CH (1996) Ind Eng Chem Res 35:864
16. Greenstein T (1980) J Mech Eng Sci 22:243
17. Chu CP, Lee DJ (2001) Bull College Eng, NTU 82:49
18. Wu RM, Lee DJ (1998) Chem Eng Sci 53:3571
19. Wu RM, Lee DJ (1999) Chem Eng Sci 54:5717
20. Wu RM, Lee DJ (2001) Water Res 35:3226
21. Wu RM, Lee DJ (2003) Chem Eng Sci 59:943
22. Jorand F, Zartarian F, Thomas F, Block JC, Bottero JY, Villemin G, Urbain V, Manem J (1995) Water Res 29:1639
23. Hsu JP, Hsieh YH (2002) Chem Eng Sci 57:2627
24. Hsu JP, Hsieh YH (2003) J Colloid Interface Sci 259:301
25. Hsu JP, Hsieh YH (2003) J Colloid Interface Sci 264:517
26. Hsu JP, Hsieh YH (2004) J Colloid Interface Sci 275:309
27. Hsu JP, Yeh SJ, Lee DJ (2005) J Colloid Interface Sci 292:290
28. Neale G, Epstein N, Nader W (1973) Chem Eng Sci 28:1865
29. Li DH, Ganczarczyk J (1990) Biotechnol Bioeng 35:57
30. Li DH, Ganczarczyk J (1988) Water Res 22:789
31. Clift R, Grace J, Weber ME (1978) Bubbles, drops and particles. Academic, New York
32. Chhabra RP (1993) Bubbles, drops and particles in non-Newtonian fluids. CRC Press, Florida
33. Bird RB, Stewart WE, Lightfoot EN (2002) Transport phenomena. Wiley, New York